Quarterly Progress Report

For Period

July 1 - September 30, 1965

FUNDAMENTAL STUDIES OF THE METALLURGICAL, ELECTRICAL, AND OPTICAL PROPERTIES OF GALLIUM PHOSPHIDE

Grant No. NsG-555

Prepared For

NATIONAL AERONAUTICS AND SPACE ADMINISTRATION
LEWIS RESEARCH CENTER
CLEVELAND, OHIO

Work Performed By

Solid-State Electronics Laboratories
Stanford University
Stanford, California

PROJECT 5108: A STUDY OF $GaAs_xP_{1-x}$

National Aeronautics and Space Administration
Grant NsG-555
Project Leader: G. L. Pearson
Staff: Yen-sun Chen

The object of this project is to evaluate the optical, electrical and metallurgical properties of the $GaAs_xP_{1-x}$ alloy system. Among evaluations of particular interest to us are the investigation of the crystal structure and its imperfections by the Kossel line technique and by that of the lattice absorption spectra as the mole fraction of GaAs, x, varies from 0 to 1.

Defects in $GaAs_xP_{1-x}$: A few epitaxially grown samples were etched in hot aqua regia to reveal the dislocations. The results are shown in Figs. 1a to 1e. Figs. 1a and 1b are for pure GaP and $GaAs_{.946}P_{.054}$ respectively. Figs. 1c and 1d are for a sample of $GaAs_{.97}P_{.03}$ before and after an annealing treatment which was carried out at 1169°C for 72 hours in an evacuated quartz ampoule with added As and P elements to prevent decomposition of the surface. Fig. 1e is for pure GaAs. The dislocation lines are all in <111> directions; the surfaces of these crystals are all (111)A oriented. The results shown in 1c and 1d clearly indicate that the sharp dislocation lines are nearly absent after the heat treatment. Furthermore, the invariance of the lattice absorption specra before and after the annealing treatment indicates that these are not defects due to inhomogeneities in composition. These lines are not present in GaAs and the dislocations are therefore believed to be caused by a lattice mismatch between the

GaAs substrate and the epitaxially grown alloy crystals.

A final report on this project is in preparation.

FIGURE CAPTION

Fig. 1 Dislocations in epitaxially grown $GaAs_xP_{1-x}$.

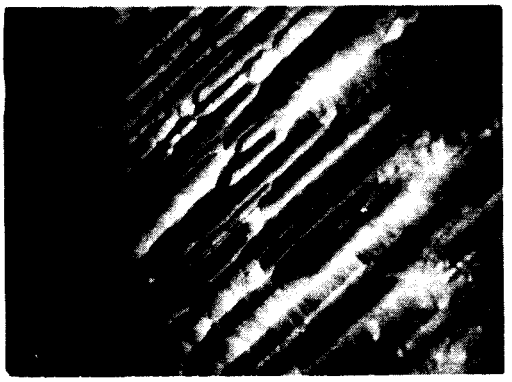

(a) GaP (X300)

(b) 5.4% P (X300)

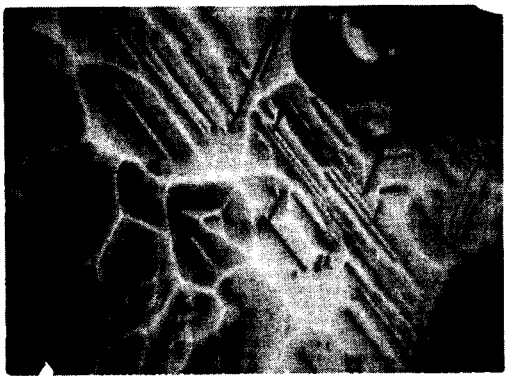

(c) 3% P BEFORE ANNEALING (X300)

(d) 3% P AFTER ANNEALING (X300)

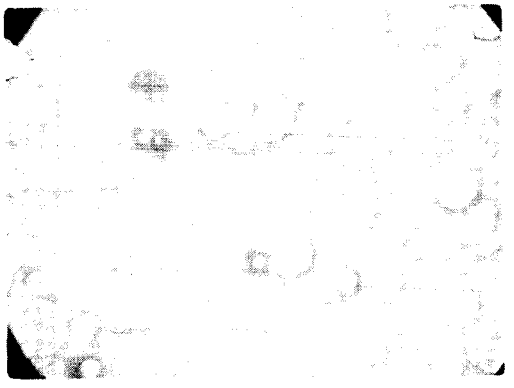

(e) GaAs (X125)

FIG. 1

PROJECT 5109: EPITAXIAL GROWTH OF III-V SEMICONDUCTOR COMPOUNDS

National Aeronautics and Space Administration
Grant NsG-555
Project Leader: G. L. Pearson
Staff: D. H. Loescher

The purpose of this project is to study the chemical, electrical and optical properties of cobalt as an impurity in gallium phosphide.

A. INTRODUCTION

This study of cobalt impurities in gallium phosphide naturally divides itself into three parts. Part one is the production of single crystals of gallium phosphide; work on crystal growth is reported in Section B. Part two is the diffusion of radiotracer cobalt into gallium phosphide in order to determine the diffusion profile and solubility of cobalt; work with radiotracer cobalt is reported in Section C. The third and final part is the measurement of the electrical and optical properties of cobalt doped gallium phosphide; this work is reported in Section D.

B. GROWTH OF GALLIUM PHOSPHIDE SINGLE CRYSTALS

During the period covered by this report nine crystal growths were performed. The important aspects of all of our crystal growths to date are summarized in Table 1. Except for the quantities N_d and Z the table should be self explanatory. N_d was calculated from the room temperature Hall coefficient, R_H, through the use of the formula for an uncompensated semiconductor

$$N_d = \frac{n^2}{5.5 \times 10^{16}} + n \qquad (1)$$

where n is given by

$$n = \frac{1}{R_H q} \quad . \qquad (2)$$

The constant 5.5×10^{16} is given by

$$5.5 \times 10^{16} = N_c \, e^{-E_d/kT} \tag{3}$$

$$= 5 \times 10^{18} \times 1.1 \times 10^{-2} \tag{4}$$

where N_c was calculated using an effective mass ratio for electrons of 0.35 and E_d was taken as 0.115 ev.[1] The quantity Z is calculated from the quantity Y, see Table 1, by dividing by the number of molecules of GaP in one cubic centimeter of gallium phosphide, i.e.,

$$Z = \frac{N_d}{(\text{S flow}/\text{P flow})(2.46 \times 10^{22})} \, . \tag{5}$$

A value of one for Z means that the ratio of sulfur to phosphorus is the same in the crystal as it was in the gas stream. A value of Z greater than one means that the sulfur to phosphorus ratio is higher in the crystal than it was in the gas stream. It has been plotted as a function of N_d in Fig. 1. While there is considerable spread in the data, it is seen that Z definitely increases as the doping is increased. It appears that the presence of sulfur in the gas stream interferes with the growth of the crystal. Since the ratio of sulfur to phosphorus in the gas stream is always quite small, see the quantity X in Table 1, it is unlikely that the sulfur ever occupies enough space in the gas to interfere physically with the phosphorous. A priori, it also seems unreasonable that the small amount of sulfur should affect the chemical reactions occurring at the substrate. However, while performing crystal growths number 13, 14 and 15 we noticed that it was necessary to grow heavily doped crystals at lower temperatures than are usual in growing lightly doped crystals.

To be specific, crystal growth 13 was performed with a substrate temperature of 815 ^{o}C and resulted in a good single crystal. The seed for growth 14 was located exactly as for number 13 but a very poor crystal, with most of the deposition occurring down stream from the seed, resulted. Growth 15 was performed at 808 ^{o}C to see if a lower substrate

temperature would solve the problem of growth 14. A very good single crystal grew on the 808 ^{o}C substrate. Following this lead we also found that the undoped crystal grown in number 12 was about 4 mils thicker than either of the lightly doped crystals number 11 or 13. Taken together the results of growths 11 through 15 strongly suggest that sulfur in the gas stream interfers with the deposition of GaP. Now consider Fig. 1 in the light of these last observations. Figure 1 is qualitatively explained if we assume that the rate of sulfur capture by the growing crystal is a linear function of the sulfur flow and use the fact that the rate of crystal growth is inversely related to the sulfur flow. A quantitative analysis of Fig. 1 is beyond the scope of this project. In summary, nine crystals were grown during the quarter. The results show that the rate of deposition of the GaP crystal is strongly influenced by the presence of sulfur in the gas stream.

C. RADIOTRACER RESULTS

Diffusion profiles have been measured on crystals 500 microns thick using the radiotracer techniques described in the last quarterly report. The results of the measurements are presented graphically in Fig. 2. A profile previously measured on a thinner sample has been included on the graph for reference purposes. On the basis of the early data, obtained using thin samples, we had concluded that cobalt diffuses quite rapidly and with a very flat profile. The more recent data shows that the profile is not perfectly flat. Consider the profiles shown in Fig. 2 in detail. All of the profiles consist of a region of rapidly decreasing concentration followed by a relatively flat region. As expected, the flat region becomes progressively flatter as the diffusion time is increased. Also the cobalt concentration increases as the diffusion time is increased. Figure 3 presents some previous results which show that the profile near the surface does not change for diffusion times longer than 7 hours. Consequently the cobalt concentration shown for the 17 hour diffusion should be very close to the solubility of cobalt in gallium phosphide at 1100 ^{o}C and 1 atmosphere phosphorus pressure. This conclusion is supported by the fact that the cobalt concentration

changes by only a factor of two between 100 microns below the surface and 500 microns below the surface. Measurements which have been made to determine whether the cobalt ends up on interstitial or substitutional sites are reported in Section D.

The diffusion profiles given in Fig. 2 show that thick crystals of gallium phosphide can be doped nearly uniformly with cobalt by diffusion; the steep part of the profile can be easily lapped away from the surface of the diffused crystal. Since a major part of this project involves studying the properties of cobalt doped gallium phosphide, this last fact is extremely useful. On the other hand, the shape of the profile would probably cause trouble in the fabrication of p-n junction devices. Also, regrettably, the cobalt concentration obtainable as a result of either short time or low temperature diffusions, conditions which yield more rounded profiles,[2] is too low to be useful for most applications.

D. ELECTRICAL AND OPTICAL MEASUREMENTS

The resistivity of cobalt diffused gallium phosphide has been measured as a function of temperature. The resistivity was measured using Hall bars, which were typically 3mm long, 1.1 mm wide and 0.25 mm thick, onto which 99 percent tin-1 percent zinc contacts had been alloyed. The equipment and method used to obtain the measurements are described in Ref. 3. The bars were cut from crystals which had been lapped, as mentioned above, after having been diffused with cobalt. The results of resistivity measurements on three samples are shown in Fig. 4. As shown in Table 1, the crystal S#11 had a room temperature carrier concentration of 6×10^{16} and crystal S#12 was undoped. The only reliable Hall measurement, which was made at room temperature on the 1115 ^{o}C-48 hr bar, yielded $p = 4.4 \times 10^{13}$ holes per cc and a mobility of 81 cm^2/volt-sec. Contact difficulties have so far prevented the measurement of the Hall coefficient on any other sample. The one measurement does confirm the hypothesis that cobalt is an acceptor in gallium phosphide. The measurements shown in Fig. 4 are discussed below. The conclusion drawn from the discussion is that additional measurements are needed to understand these data.

The results of Fermi-Dirac statistics needed to discuss Fig. 4 are given below. Consider a crystal at temperature T containing N_A acceptors, N_D donors, and p holes. Then

$$N_A - N_D = p + N_A \left(1 - \frac{1}{e^{\frac{E_A - E_f}{kT}} - 1} \right) \tag{6}$$

and

$$p = N_V e^{-E_f/kT} \tag{7}$$

giving

$$N_V e^{-E_A/kT} = \frac{p(p + N_D)}{N_A - N_D - p} , \tag{8}$$

where N_V is the effective density of valence band states and E_f is the Fermi energy, all energies being measured upward from the valence band. The largest room temperature value of p calculated from the data in Fig. 4 is 3.4×10^{13} holes/cc. An estimate of N_d, obtained from the resistivity of sample S#12, is 2.6×10^{14}, i.e., about an order of magnitude larger than p. Consequently we can rewrite Eq. (8) in the approximate form

$$N_V e^{-E_A/kT} \simeq \frac{p\, N_D}{N_A - N_D} , \tag{9}$$

which leads to

$$\ln p = \ln \frac{N_V(N_A - N_D)}{N_D} - \frac{E_A}{kT} \tag{10}$$

and

$$\frac{d \ln \rho}{d \frac{1}{T}} = - \frac{E_A}{k} . \tag{11}$$

if the temperature variation of mobility compensates that of N_V. Equation (11) shows that the slope of the lines in Fig. 4 should correspond to the activation energy of cobalt.

Equations (7) and (9) yield the result that

$$E_f = E_A + kT \ln \frac{N_D}{N_A} \tag{12}$$

Since N_D is less than N_A the Fermi level will always lie below the acceptor level, remember however that the formula only applies as long as N_D is larger than p. As a consequence of Eq. (12), any measurement of resistivity should yield a smaller value than would be obtained using the formula

$$\rho = \frac{1}{q\mu N_V} e^{E_A/kT} \tag{13}$$

where μ is the mobility and q is the electronic charge. In Fig. 5 p from Eq. (7) and ρ from Eq. (13) are plotted as functions of E_f (or E_A). The graph was calculated using $\mu = 81$ cm^2/volt-sec and an effective mass ratio for holes of 0.8, as suggested by Allen and Cherry.[4]

Now compare the data shown in Fig. 4 with the calculations given in Fig. 5. The sample with an activation energy of 0.25 eV had a room temperature resistivity of 4×10^3 ohm-cm. Figure 5 shows that for $E_f = 0.2$ eV the resistivity should be about 60 ohm-cm. Similarly the 0.32 eV sample was 2.1×10^3 ohm-cm at room temperature while for 0.32 eV, Fig. 5 gives about 1000 ohm-cm. Finally for the 0.38 eV sample the values are 8×10^4 ohm-cm and about 10^4 ohm-cm respectively. Since, as discussed above, the Fermi level lies below E_A for any reasonable ratio of N_D to N_A, the measured resistivity should be lower, not higher, than that predicted from Fig. 5. The reason for the anomalously high measured resistivity is not known.

Besides the difficulty with the actual value of the resistivity shown in Fig. 9 there is a problem with the activation energies. One can imagine at least four electrical states for cobalt in gallium phosphide, singly and doubly charged cobalt on either interstitial or substitutional sites, and each could have a different activation energy. However, as the diffusion conditions for the 0.25 eV and 0.32 eV samples were very

nearly the same, cobalt should be distributed about the same in both cases. Clearly another tool is needed to determine where the cobalt is in the crystal and how it is distributed. The combination of optical absorption measurements and crystal field theory gives us such a tool. The result of using this tool, which is discussed in detail below, is that after a 48 hour 1200 ^{o}C diffusion most of the cobalt is on substitutional sites. Consequently the value of 0.38 ev is tentatively assigned to substitutional cobalt. Also notice that at high temperatures the slopes of 0.25 ev and 0.32 ev samples change to approximately 0.36 ev. This last observation suggests that after diffusions at the lower temperatures some of the cobalt is on substitutional sites, where the activation is 0.38 ev, and some is on interstitial sites where the activation energy is lower. More experiments will allow us to determine the cause of the anomalously high resistivity and to sort out the multiple activation energies.

A combination of an optical absorption measurement and crystal field theory has been used to determine the location of the cobalt impurities in gallium phosphide in which cobalt was diffused at 1200 ^{o}C for 39 hrs. The absorption measurements were made at 77 ^{o}K using a Cary Model 14 1R recording spectrophotometer. The model 14 1R is a modified version of the model 14 which allows measurements to be made out to 1.7 microns with the visible range light beam configuration. In order to obtain sufficient absorption it was necessary to stack two diffused pieces, one on top of the other, in the sample chamber. The effects of multiple reflections and background absorption were removed when the traces from the Cary were read. The results of plotting the absorption coefficient due to the cobalt, as a function of wave number, are shown in Fig. 7. The conclusion of the detailed discussion of Fig. 7 given below is that the absorption peaks are due to substitutional cobalt.

The effect of ligand atoms on the atomic levels of a central atom is treated in crystal field theory. The subject, which was originally developed by Bethe,[5] has been treated recently by Ballhausen[6] and McClure.[7] Basically the theory consists of the use of perturbation theory and group theory to calculate the effects of lowering the symmetry of the atomic environment. As an example of the theory, consider

the splitting of the cobalt d-shell in a tetrahedral field. Cobalt has the electronic configuration $[A]\ 3d^7 4s^2$ where $[A]$ represents the filled argon shells. There are

$$\frac{10 \cdot 9 \cdot\cdot 8}{1 \cdot 2 \cdot 3} = 120 \tag{14}$$

ways of putting seven electrons into ten levels. Due to electron-electron interaction this 120-fold degeneracy is partially lifted. The effects of electron-electron interaction can be calculated using multiplet theory[6,7] and are listed in Ref. 6 (page 24). The result of multiplet theory is that the lowest state for 7 3d electrons is a 28 fold degenerate ^4F state; the notation is the logical extension of the single electron notation with an added presuperscript to give the spin degeneracy. The second lowest state is ^4P which is 12-fold degenerate and lies 15B, where B is the Racah parameter, above ^4F. The relative energies of the lower states of 7 3d electrons are shown along the ordinate in Fig. 7. When the cobalt atom is put into a tetrahedral field some of the multiplet degeneracy is lifted. For example, the ^4F state splits into a $^4A_2$, a $^4T_1$, and a $^4T_2$ state; here Mulliken's notation for the irreduci representations of the group T_d is used. In this notation A represents a singlet state, E a doublet, and T a triplet. Note that the number of split states

$$4 \cdot 1(^4A_2) + 4 \cdot 3(^4T_1) + 4 \cdot 3(^4T_2) = 28 \tag{15}$$

equals the number of original states

$$4 \cdot (2 \cdot 3 + 1)(^4F) = 28 \tag{16}$$

as it must. The splittings of the lower states of 7 3d electrons are shown in Fig. 6 as a function of the crystal field parameter Dq. Dq, which is generally treated as an empirical quantity, measures the strength of the crystal field. Symmetry and quantum selection rules show that electric dipole transitions from $^4A_2(^4F)$ to $4T_1(4F)$ and

from $^4A_2(^4F)$ to $^4T_1(^4P)$ are allowed if there is some mixing between the d cobalt states and p states of the ligands. This mixing is necessary because electric dipole transitions are forbidden between two pure d-states. Also, since there should be more mixing between the excited state ^4P and the ligands than between the ground state and the ligands, the $^4A_2(^4E) - {}^4T_1(^4P)$ transition should be stronger than the $^4A_2(^4F) - {}^4T_1(^4F)$ transition. Finally, notice that near $Dq/B = 0.3$, there should be considerable mixing between ^4P and the split states of ^2G. The interpretation of the experimental results in Fig. 6 is now straightforward.

The absorption peak near 8200 cm^{-1} is caused by the $^4A_2(^4F) - {}^4T_1(^4F)$ transition. The peak near 12,500 cm^{-1} is caused by the $^4A_2(^4F) - {}^4T_1(^4P)$ transition. The structure on the latter peak is caused by the mixing of ^4P and ^2G states near $Dq/B = 0.3$. The oscillator strengths for the two transitions have been calculated using the formula:[9]

$$Nf_{12} = \frac{nm^*c}{2\pi^2 e^2 \hbar} \left(\frac{E_o}{E_{eff}}\right)^2 \int \mu_{12}(E)\, dE \,, \qquad (15)$$

where N is the concentration of impurities in atoms per cc, n is the index of refraction, m^* is the effective mass, $\hbar$ is Planck's constant in units of ev-sec, μ_{12} is the absorption constant in cm^{-1}, E is energy in eV, and (E_o/E_{eff}) is the effective field ratio. After inserting the values of the constants appropriate to gallium phosphide and setting $(E_o/E_{eff}) = 1$ Eq. (15) becomes

$$Nf_{12} = 2.67 \times 10^{16} \int \mu_{12}(E)\, dE \,. \qquad (16)$$

The results of applying equation (16) to Fig. 6 are

$$f_{8200} \cong 8.7 \times 10^{-4}$$

$$f_{12500} \cong 4.8 \times 10^{-3}$$

and

$$\frac{f_{12500}}{f_{8200}} = 5.5$$

These values of f are about ten times larger than those expected for cobalt in a centrosymmetric octahedral field. This last fact combined with the fact that the absorption spectrum of octahedrally coordinated cobalt would be significantly different from the spectrum should in Fig. 7 prove conclusively that the cobalt in the crystal measured is on tetrahedral sites. Further consideration leads to a second very important conclusion, namely that the cobalt has the $3d^7$ configuration and has not become $3d^6$ in the process of substituting for gallium. To summarize, the application of crystal field theory to the spectrum of Fig. 7 shows that the cobalt atoms in the sample measured were on substitutional sites and have the $3d^7$ inner shell configuration. Absorption measurements will be made on sample diffused at other temperatures in the future.

The combination of optical absorption and crystal field theory is potentially a very powerful tool. To date this method of studying transition metals has been used only by inorganic chemists studying compounds which could contain large amounts of the metal as an impurity. Our measurements show that impurity concentrations as low as a few times 10^{17} can be detected. Moreover, since sensitive spectrophotometers are fairly common, it is possible to use quite small samples. The stacked crystal used in our measurement was about 3mm × 2mm × 1mm and contained a total of about 10^{15} cobalt atoms. This last number is about an order of magnitude below the limit of detectability for most EPR measurements. Summarizing, one optical absorption measurement made at 77 °K has yielded information about site symmetry and electron configuration which could not have been obtained by any other means.

E. CONCLUSION

On the basis of the work performed during the last quarter we conclude:

1. That the presence of sulfur in the gas stream during expitaxial growth reduces the growth rate.
2. That it is possible to obtain nearly uniform samples of Co-doped GaP by solid state diffusion.
3. That Co is a complicated acceptor in GaP.
4. That Co with a $3d^7$ electronic configuration is located on substitutional sites after a 39 hour diffusion at 1200 °C.

REFERENCES

1. T. S. Moss, "Infra-Red Faraday Effect Measurements on GaP and AlSb," Proc. of the International Conference on the Physics of Semiconductors, Exeter, Jul 1962, p. 295-300.

2. D. Loescher, SEL Quarterly Research Review No. 13, in preparation.

3. Quarterly Research Review No. 12, Stanford Electronics Laboratories, p. II-50-52.

4. J. W. Allen and Cherry, J. of Phys. and Chem. of Solids, 23, 163, Jan-Feb 1962.

5. H. Bethe, Ann. Physik, 5, 3, 135, 1929.

6. C. J. Ballhausen, Introduction to Ligand Field Theory, McGraw-Hill Book Company, New York, 1962.

7. D. S. McClure, Electronic Spectra of Molecules and Ions in Crystals, Academic Press, New York, 1959.

8. J. C. Slater, Quantum Theory of Atomic Structure, McGraw-Hill Book Company, New York, 1960, Vol. I.

9. D. L. Dexter, Solid State Physics, Academic Press, New York, 1958, Vol. 6, p. 370.

TABLE I

GROWING CONDITIONS AND CARRIER DENSITIES OF SULFUR DOPED GaP SINGLE CRYSTALS

Sample	N_d cm^{-3}	S moles/min	P moles/min	X = S/P	$Y = N_d/X$	Z
1	5.3×10^{18}	2.0×10^{-9}	7.2×10^{-5}	2.8×10^{-5}	1.9×10^{23}	7.7
2	1.7×10^{17}	4.9×10^{-10}	7.2×10^{-5}	6.8×10^{-6}	2.5×10^{22}	1
3	1.8×10^{20}	1.9×10^{-8}	1.2×10^{-4}	1.6×10^{-4}	1.1×10^{24}	4.5
4	4.2×10^{19}	5.4×10^{-9}	1.2×10^{-4}	4.2×10^{-5}	1.0×10^{24}	41
5	3.4×10^{17}	1.8×10^{-10}	7.2×10^{-5}	2.5×10^{-6}	1.4×10^{23}	5.7
6	2.7×10^{17}	6.7×10^{-10}	7.2×10^{-5}	9.3×10^{-6}	2.9×10^{22}	1.2
7	N.M.*	1.8×10^{-9}	7.2×10^{-5}	Good Crystal		
8	4.8×10^{19}	6.6×10^{-10}	7.2×10^{-5}	9.2×10^{-6}	5.2×10^{24}	210
9		Polycrystal Due To Mislocation Of Seed				
10	N.M.	0	$\rho_{300^oK} = 8\times10^{4}$ ohm-cm			
11	1.2×10^{17}	6.7×10^{-10}	7.2×10^{-5}	9.3×10^{-6}	1.3×10^{22}	.53
12	N.M.	0	$\rho_{300^oK} = 590$ ohm-cm			
13	N.M.	1.8×10^{-10}	Good Crystal			
14	N.M.	9.24×10^{-10}	Poor Crystal			
15	N.M.	9.24×10^{-10}	Good Crystal			

* N.M. means that the value has not been measured.

FIGURE CAPTIONS

Fig. 1 The quantity z (see text and Table I) as a function of the sulfur doping N_D.

Fig. 2 Co profiles in GaP after 1109°C diffusions at a phosphorus pressure of approximately 1 atmosphere and for the times indicated.

Fig. 3 The results of 1015°C diffusions for 7, 24, and 50 hours.

Fig. 4 The resistivity of Co doped gallium phosphide is shown as a function of temperature. The diffusion conditions are as indicated.

Fig. 5 The room temperature hole concentration and resistivity are shown as a function of E_f. The value 81 cm^2/volt-sec was used for the mobility.

Fig. 6 The crystal field splitting of the Co d-shell is shown as a function of the parameter D_q. All energies are in units of B. The symmetry classification of the different states is given in Bethe's notation.

Fig. 7 The experimentally measured absorption due to cobalt d-shell transitions is shown as a function of wave number.

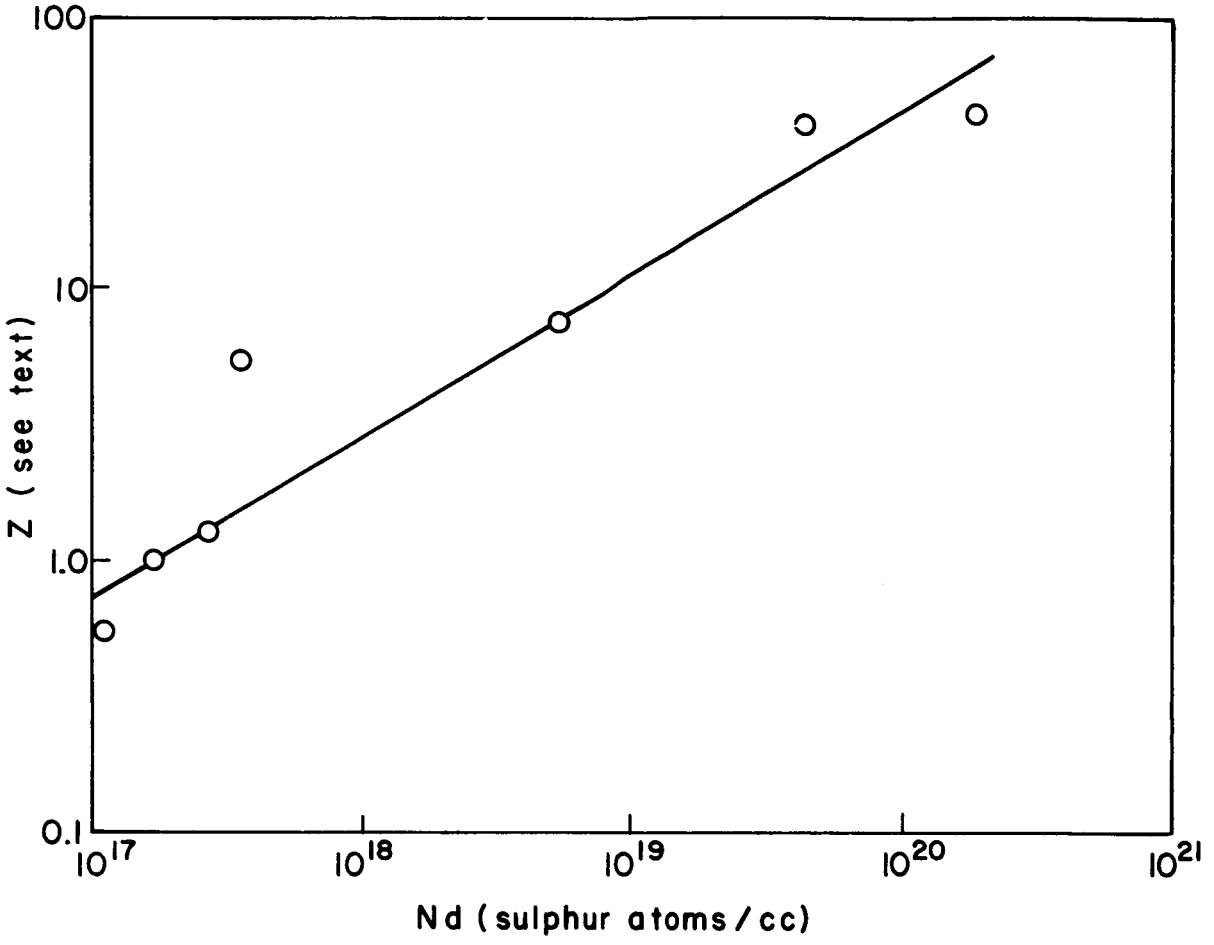
100
10
1.0
0.1
Z (see text)
10^{17}
10^{18}
10^{19}
10^{20}
10^{21}
Nd (sulphur atoms / cc)

FIG. 1

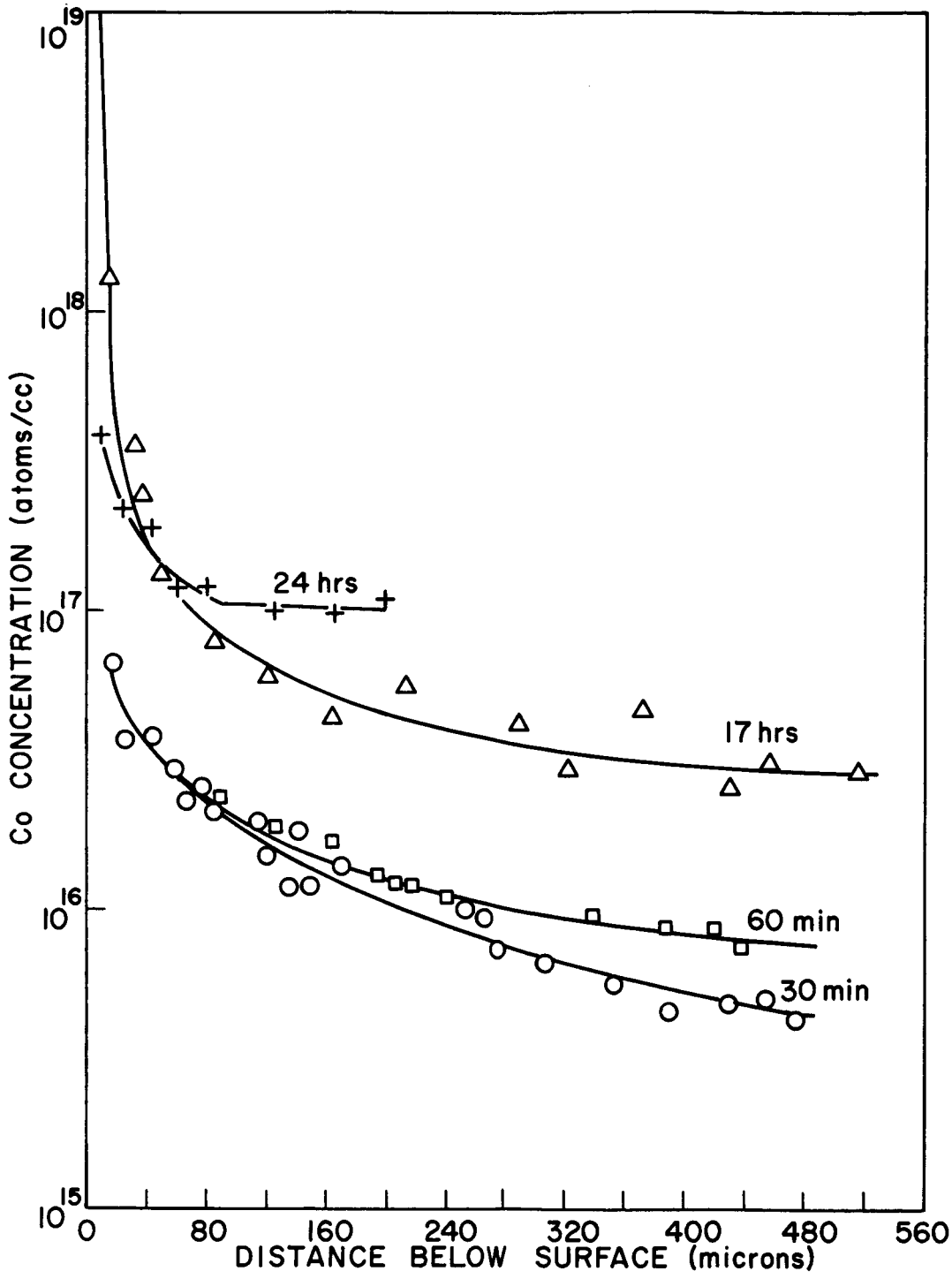
Co CONCENTRATION (atoms/cc)
10^19
10^18
10^17
10^16
10^15
24 hrs
17 hrs
60 min
30 min
0
80
160
240
320
400
480
560
DISTANCE BELOW SURFACE (microns)

FIG. 2

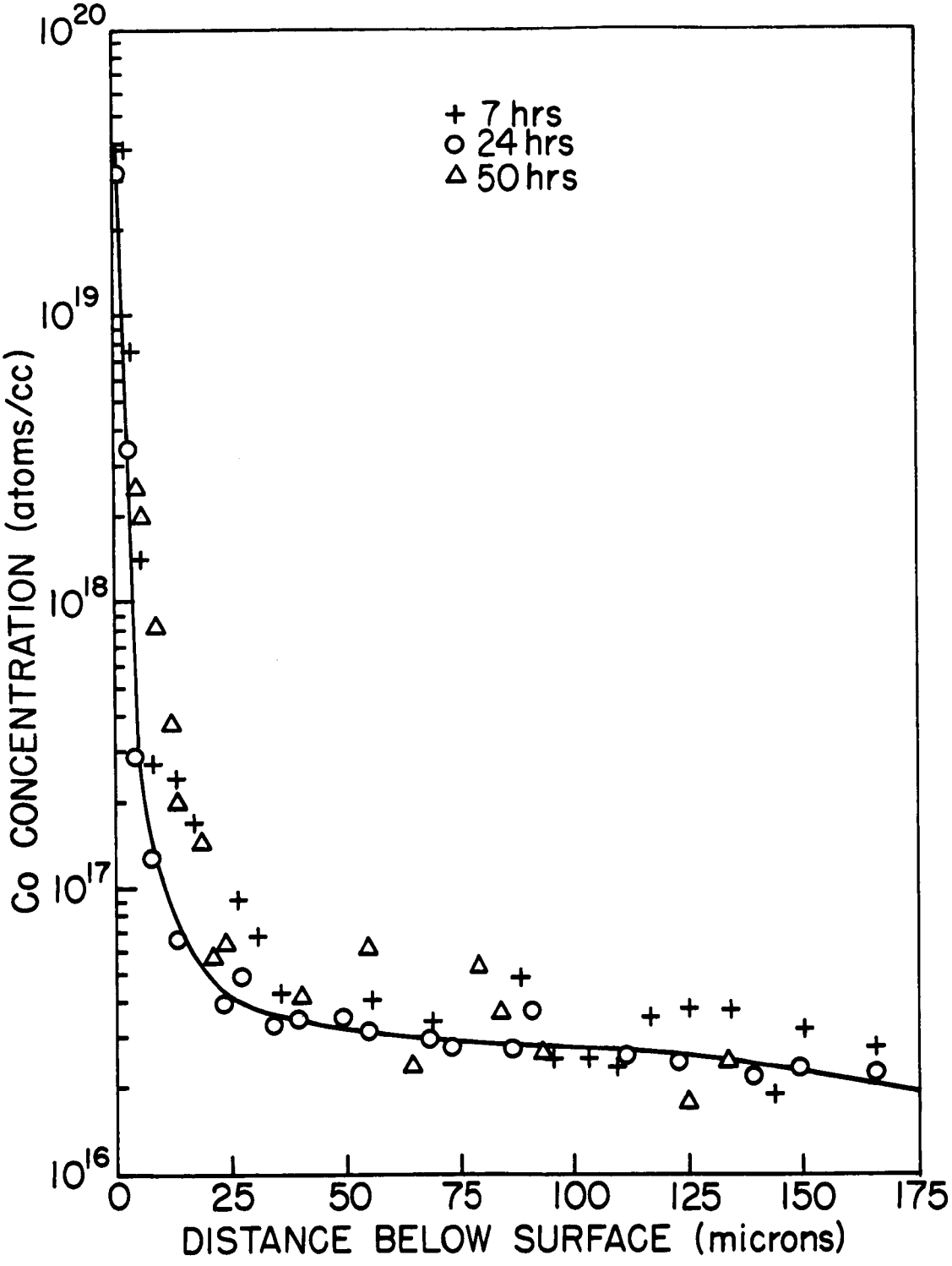
+ 7 hrs
o 24 hrs
Δ 50 hrs
Co CONCENTRATION (atoms/cc)
10^{20}
10^{19}
10^{18}
10^{17}
10^{16}
0
25
50
75
100
125
150
175
DISTANCE BELOW SURFACE (microns)

FIG. 3

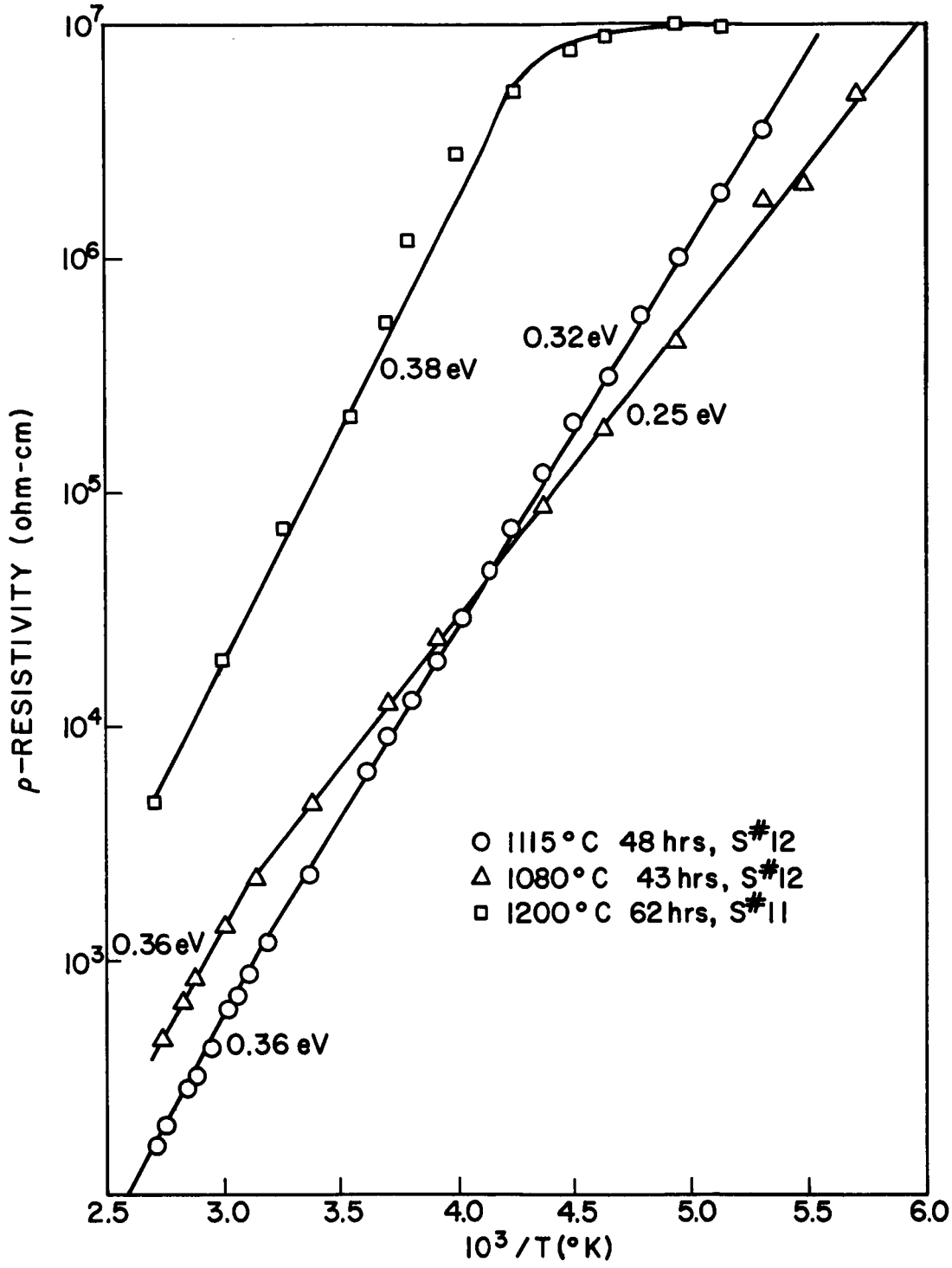
10^7
10^6
10^5
10^4
10^3
ρ-RESISTIVITY (ohm-cm)
0.38 eV
0.32 eV
0.25 eV
0.36 eV
0.36 eV
○ 1115°C 48 hrs, S#12
△ 1080°C 43 hrs, S#12
□ 1200°C 62 hrs, S#11
2.5
3.0
3.5
4.0
4.5
5.0
5.5
6.0
10^3/T (°K)

FIG. 4

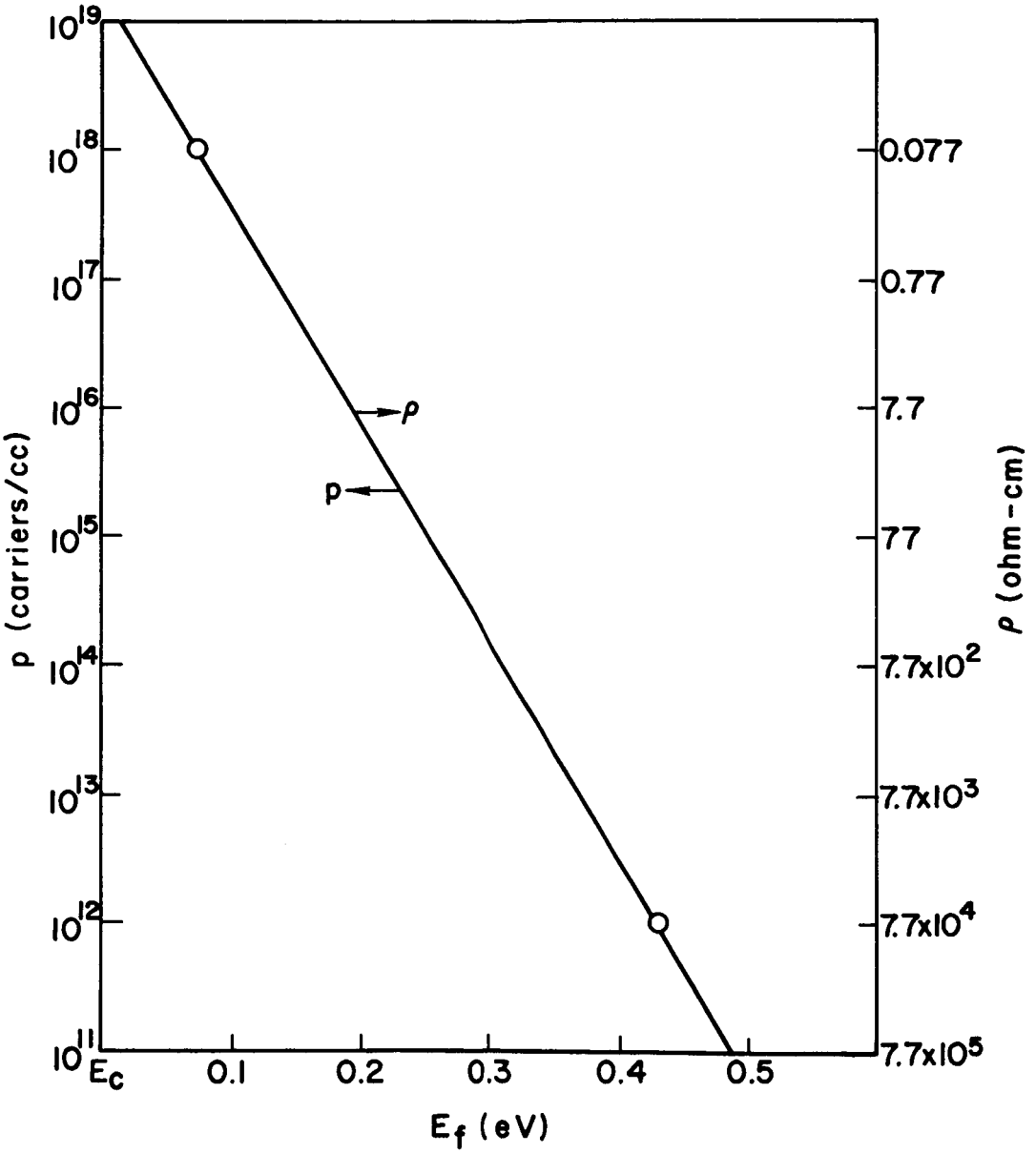
10^{19}
10^{18}
10^{17}
10^{16}
10^{15}
10^{14}
10^{13}
10^{12}
10^{11}
p (carriers/cc)
ρ
p
0.077
0.77
7.7
77
7.7×10^{2}
7.7×10^{3}
7.7×10^{4}
7.7×10^{5}
ρ (ohm-cm)
E_c
0.1
0.2
0.3
0.4
0.5
E_f (eV)

FIG. 5

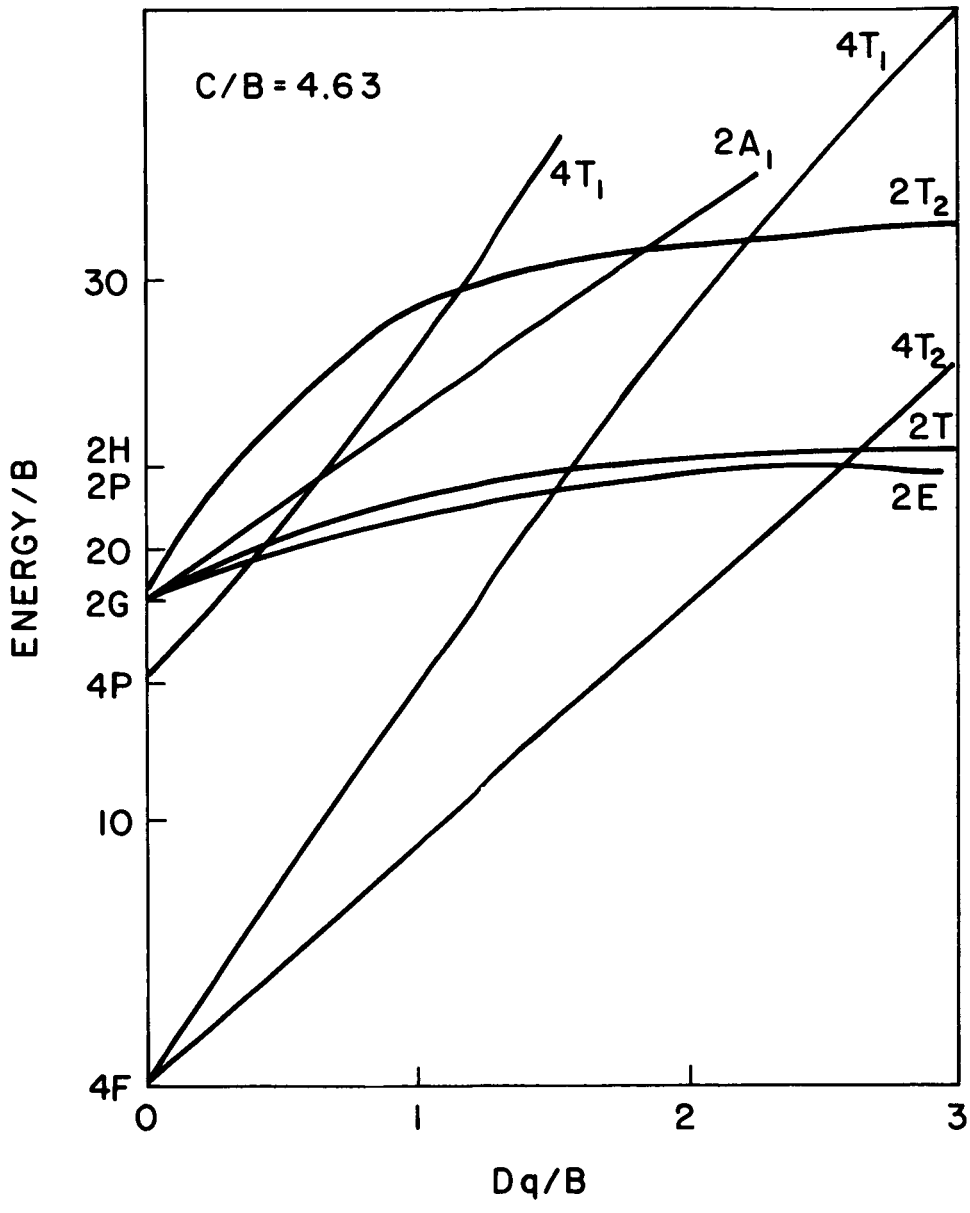
C/B = 4.63
4T1
2A1
4T1
2T2
4T2
2T
2E
30
2H
2P
20
2G
4P
10
4F
ENERGY/B
0
1
2
3
Dq/B

FIG. 6

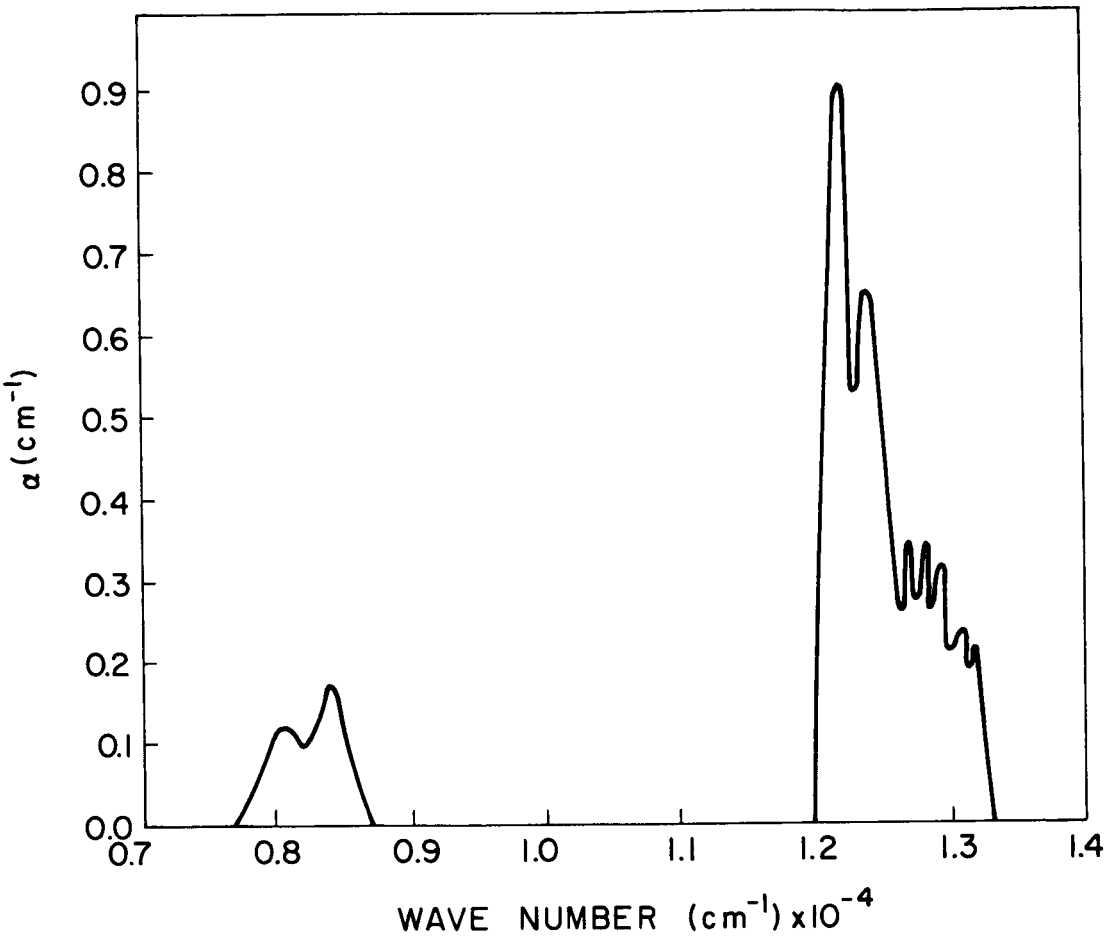
0.9
0.8
0.7
0.6
0.5
0.4
0.3
0.2
0.1
0.0
α (cm⁻¹)
0.7
0.8
0.9
1.0
1.1
1.2
1.3
1.4
WAVE NUMBER (cm⁻¹) x10⁻⁴

FIG. 7

Project 5112: THE PROPERTIES OF RECTIFYING JUNCTIONS IN $GaAs_xP_{(1-x)}$

National Aeronautics and Space Administration Grant NsG-555
Project Leader: G. L. Pearson, J. L. Moll
Staff: T. Koike

The purpose of this project is to study the properties of rectifying junctions in GaP and $GaAs_xP_{(1-x)}$. It is planned to investigate both metal barriers and p-n junctions.

A. INTRODUCTION

During the last quarter a few more sulfur-doped n-type GaP single crystals were grown under different growing conditions in order to obtain different doping levels for our single crystals. Several alloyed p-n junctions were fabricated from one of the grown crystals and the forward characteristics of these were studied in detail.

The study of photovoltaic cells constructed from n-type GaP was also started and some characteristics of the first cell are given in this report.

B. CRYSTAL GROWTH

Two sulfur-doped n-type GaP single crystals were grown by the open tube method.[1] In order to obtain two different doping densities (10^{16} cm^{-3} and 10^{17} cm^{-3}), sulfur was kept in boiling baths of acetone (b.p. = 56.5 °C) and methanol (b.p. = 64.65 °C).[2] The growth conditions are summarized in Table 1. In both both growths, single crystals greater than 30 mils in thickness were obtained.

C. PROPERTIES OF ALLOYED pn JUNCTIONS

A few alloyed pn junctions were made according to the process described in the previous report[3] from the n-type GaP single crystal ($N_D = 3 \times 10^{16}$ cm^{-3}) grown in the previous quarter. A tin pellet was alloyed for 5 min and after a brief etching in aqua regia (10 sec) a tin (99 percent) - zinc (1 percent) dot was alloyed for 10 min in the Marshall furnace at 500 °C with a hydrogen flow rate of 1 cu ft/hr.

TABLE 1. GROWTH CONDITIONS FOR SULFUR-DOPED n-TYPE GaP SINGLE CRYSTALS

Run Number		J-29	J-31
Substrate (GaAs)	Temperature °C	820	820
	Temperature Gradient °C/cm	16	16
	Orientation	(111)	(111)
	Angle Against Flow	30°	30°
Flow of H_2	By Pass cc/min	80	46
	PCl_3(0 °C) cc/min	57	57
	Doping Line (sulfur) cc/min	8.2	39.2
Boiling Liquid Bath		Acetone (56.5 °C)	Methanol (64.65 °C)
Donor Density (expected) cm^{-3}		$\sim 10^{16}$	$\sim 10^{17}$

A typical V-I curve of Diode D-7-25 is shown in Fig. 1a. The same diode was later given a special treatment which consisted of etching for 1 min in a $1HCl - 2HNO_3$ solution and baking for 30 min in an oven kept at 100 °C. A slight improvement in the reverse breakdown characteristics is evident after the treatment as shown in Fig. 1b. It should also be noticed that the reverse breakdown voltage is fairly consistent with that of Diode A reported in the previous quarter.[3] Both diodes were fabricated under identical conditions from the same crystal.

The detailed forward characteristics were measured before and after the baking treatment and the results indicated some interesting features as shown in Fig. 2. In either case the forward characteristics do not follow the simple recombination-generation model described by Sah, Noyce, and Shockley.[4] There is a considerable amount of excessive current at low bias voltages. So far our study has not shown any conclusive evidence regarding the source of this excessive current. However, the increase in the forward current at low bias voltages after the treatment may indicate that a part of the excessive current is due to the surface condition as noted in the previous report.[3]

At higher bias voltages the diode current is affected by the series resistance which is about one order of magnitude higher than the expected value. Since there is no anomalous resistance at the ohmic contact,[3] there may be two possible reasons for this anomalous resistance. One is the imperfect alloying of the pn junction and the smaller effective area of the pn junction. Another is the existence of a highly compensated (near intrinsic) region near the pn junction. If we examine the junction capacitance at zero bias, we find that in either Diode B (reported in the previous report[3]) or D-7-25 the capacitance is one order of magnitude smaller than expected. From this evidence and additional evidence which will be mentioned later, the latter seems to be the main reason for the anomaly in the series resistance.

D. GALLIUM PHOSPHIDE SOLAR CELLS

GaP photovoltaic cells were fabricated from the grown single crystal and some measurements were performed on the cells. The details are reported below.

1. Solar Cell Fabrication

Crystal J-29 was cut into a small piece and lapped and polished. Then the sample was etched in a $2HNO_3$ - 1HCl solution for 5 min. After the etching was done, the sample was sealed in a closed ampule with 1 mg of Zn (9.9999 percent) evacuated to less than 10^{-3} mmHg. It was very important to separate the crystal from the Zn pellet, so that the special shape of the ampoule was needed as shown in Fig. 3. The volume of the ampoule was about 2.5 cm^3.

The diffusion of Zn into GaP is not described by the simple diffusion theory in which the diffusion coefficient is assumed constant. It has been established by Chang[5] that the diffusion of Zn in GaP is described by the parallel-mode model in which both interstitial and substitutional diffusions take place. This results in a sharper diffusion front than the prediction of the complementary error function. Therefore, the exact calculation of the diffusion time is difficult.

However, Chang[5] reported about 12μ for the diffused layer thickness as a result of one hour diffusion at 800 °C. We decided to perform the diffusion at 800 °C for less than one hour to obtain a thinner diffused layer. The actual diffusion was done at 800 °C for 13 min.

After the diffusion the ampoule was quickly quenched in cold water, to minimize the deposition of Zn from the vapor. Then, the sample was examined under the microscope. It was found that Zn tended to deposit at surface damage scratches and dislocations revealed by etching prior to the diffusion. This is shown in Fig. 4. The sample was then washed in a 1HCl - 1H_2O solution for 5 min to remove free Zn from the surface.[5] Some of the Zn deposits were not affected by this treatment. This may indicate that a Zn - GaP alloy was formed at these spots and that the diffused layer thickness was not uniform. This was partly confirmed by a grooving thechnique.[6] The boundary between the Zn-diffused region (dark) and the n-type GaP (light) was not clear under the microscope. However, an approximate junction depth of about 5μ was obtained. This also indicated that the diffusion condition was in the proper range. A technique to indicate the junction depth clearly should established to study this in detail.

After the above treatment one side of the sample was lapped and polished to reveal the n-type surface. A thermoelectric probe showed that the diffused surface was p-type, and the polished surface was n-type. Then, a tin ohmic contact on the n-side and a Sn + 1 percent Zn contact on the p-side were alloyed in the hydrogen furnace for 5 min with a hydrogen flow rate of 1 cu ft/hr. The dimension of the sample (PC-8-17) is shown in Fig. 5.

2. V-I Characteristics

The current-voltage characteristics of PC-8-17 at room temperature is shown in Fig. 6. The reverse breakdown was very soft. It was also noticed that the series resistance was still too large for the dimension of the crystal.

3. Optical Measurement

Spectral response measurements were made on a Bausch and Lomb monochromator with a tungsten light source and a HP 425-A. The experimental setup is illustrated in Fig. 7. The solar cell was mounted at the exit of the monochromator and a constant exit slit width of 5 mm was maintained throughout the measurement. The result is shown in Fig. 8 without correction. The maximum response was observed at $\lambda = 0.492\mu$. However, another peak at 0.7μ observed by some workers[7,8] was not detected.

4. E-I Power Curve

The E-I power curve was obtained in sunlight for cell PC-8-17 at 23 °C. The result is shown in Fig. 9. The conversion efficiency is about 0.2 percent if an input power of 100 MW/cm^2 is assumed. The open circuit voltage of this cell (PC-8-17) was 0.58 volts. This was considerably lower than the value obtained by other workers.[7,8]

5. Remarks

Although the solar cell (PC-8-17) was not particularly designed to optimize the operation, it disclosed some interesting features. First of all, the 0.7μ peak was not found in the cell (PC-8-17). Gershenzon and Mikulyak[9] postulated a donor level due to oxygen at 0.4 ev below the conduction band and Epstein and Groves[8] postulated that this might correspond to the 0.7μ. If this is the case, although it has not been verified yet, then one of the reasons for the absence of the 0.7μ may be due to the fact that the junction depth of the cell (PC-8-17) is quite large ($\sim 5\mu$) and the main response of the cell is occurring in the p-type layer where the donor level is highly compensated by the Zn diffusion. This also seems to correspond to the small junction current and efficiency ($\sim$0.2 percent) in the cell (PC-8-17). The establishment of a technique to obtain a uniform and thin ($\sim 1\mu$) diffusion layer is needed to study this further.

Secondly, the open-circuit voltage turned out to be quite low. We have already noticed[3] that there is no anomalous resistance between the ohmic contact and the n-type bulk GaP and that the anomalous resistance exists near the p-n junction region. This leads to the speculation that a highly compensated or intrinsic region exists near the pn junction region as mentioned earlier in this report and that the voltage drop occurs in this region. Since the bulk n-type material has a relatively low donor density ($\sim 10^{16}$ cm^{-3}), this seems very likely. This result seems to be connected to the existence of a high series resistance and a low junction capacitance. Therefore, measurement of capacitance vs applied voltage relation on solar cells with various bulk donor densities will be necessary as well as the optical measurements.

Work during the next quarter will be concentrated on characterization of various parameters of the solar cell operations and improvement of the fabrication technique.

REFERENCES

1. Y. S. Chen, SEL Quarterly Research Review No. 10 and 11.

2. D. H. Loescher, SEL Quarterly Research Review No. 12.

3. T. Koike, SEL Quarterly Research Review No. 13.

4. C. T. Sah, R. N. Noyce, and W. Shockley, IRE, 45, 1228 (1957).

5. L. L. Chang, SEL Technical Report No. 5104-1 (1963).

6. B. MacDonald and A. Goetzberger, J. Elec. Chem. Soc., 109, 141 (1962).

7. H. G. Grimmeiss and H. Koelmans, Philips Res. Repts., 15, 290 (1960).

8. A. S. Epstein and W. B. Groves, Advanced Energy Conversion, 5, 161 (1965).

9. M. Gershenzon and R. M. Mikulyak, Solid-State Electron., 5, 313 (1962).

FIGURE CAPTIONS

Fig. 1. V-I Curves of Diode D-7-25. H: 1 V/div; V: 1 ma/div.

a. Before the Baking Treatment.

b. After the Baking Treatment.

Fig. 2. Detailed Forward Characteristics of Diode D-7-25 Before and After the Baking Treatment.

Fig. 3. A Schematic Drawing of the Diffusion Ampoule. Volume $\tilde{-}$ 2.5 cm^3.

Fig. 4. Deposition of Zn Along Surface Damage Scratches and at Dislocations.

Fig. 5. Dimension of the Solar Cell PC-8-17. Area = 6.9×10^{-2} cm^2.

Fig. 6. V-I Curve of Solar Cell PC-8-17. H: 1 V/div; V: 1 ma/div.

Fig. 7. Equipment for Measuring Spectral Response of Solar Cells.

Fig. 8. Spectral Response of Solar Cell PC-8-17 Without Correction.

Fig. 9. E-I Curve for PC-8-17 at Room Temperature in Sunlight.

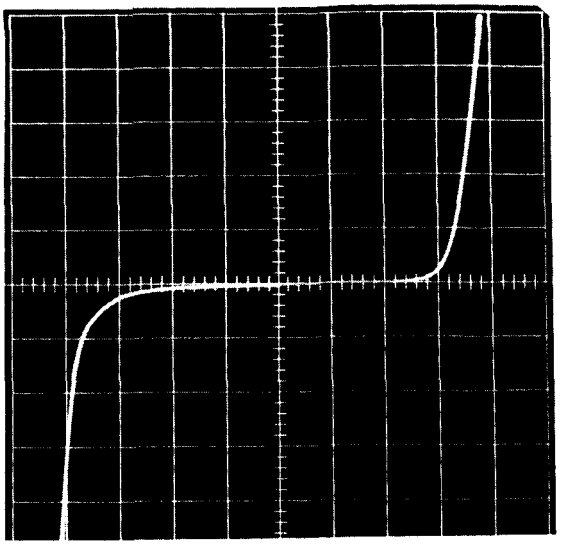

(a)

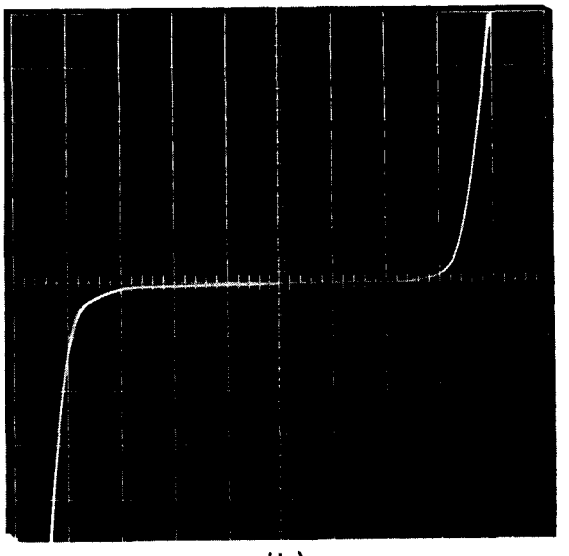

(b)

FIG. 1

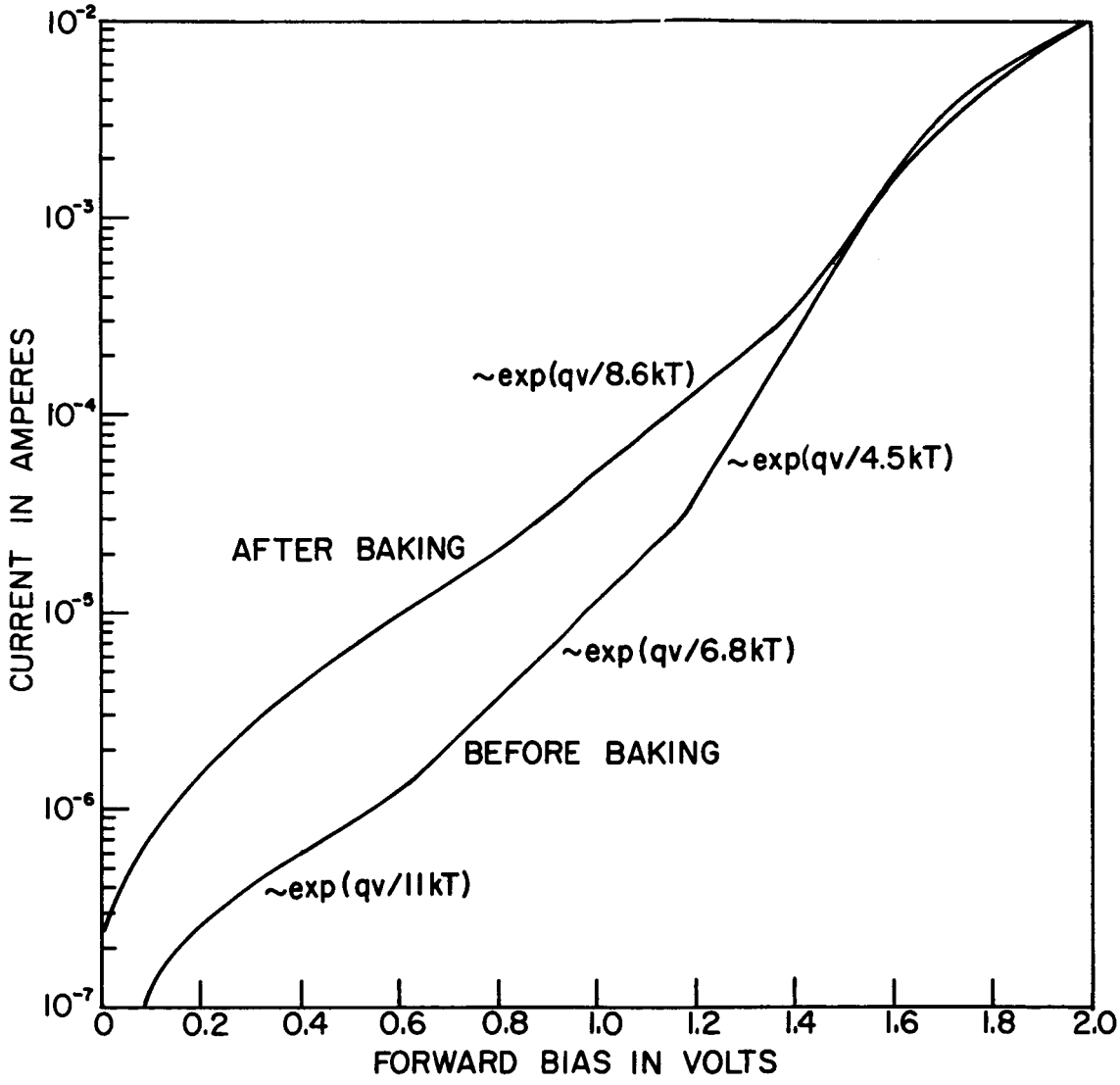
10^{-2}
10^{-3}
10^{-4}
10^{-5}
10^{-6}
10^{-7}
CURRENT IN AMPERES
~exp(qv/8.6kT)
~exp(qv/4.5kT)
AFTER BAKING
~exp(qv/6.8kT)
BEFORE BAKING
~exp(qv/11kT)
0
0.2
0.4
0.6
0.8
1.0
1.2
1.4
1.6
1.8
2.0
FORWARD BIAS IN VOLTS

FIG. 2

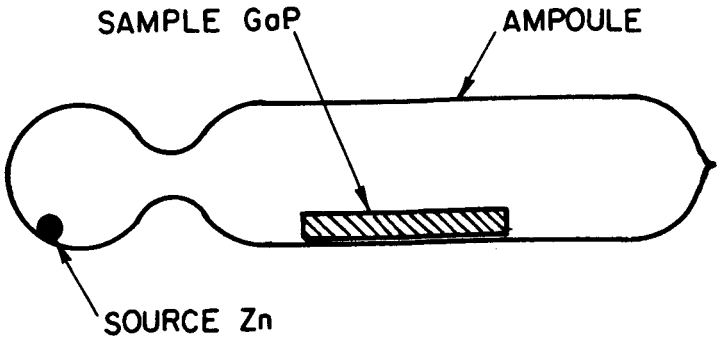

FIG. 3

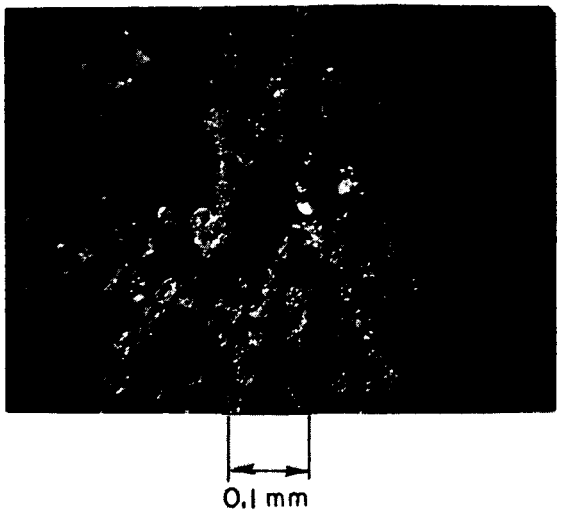

FIG. 4

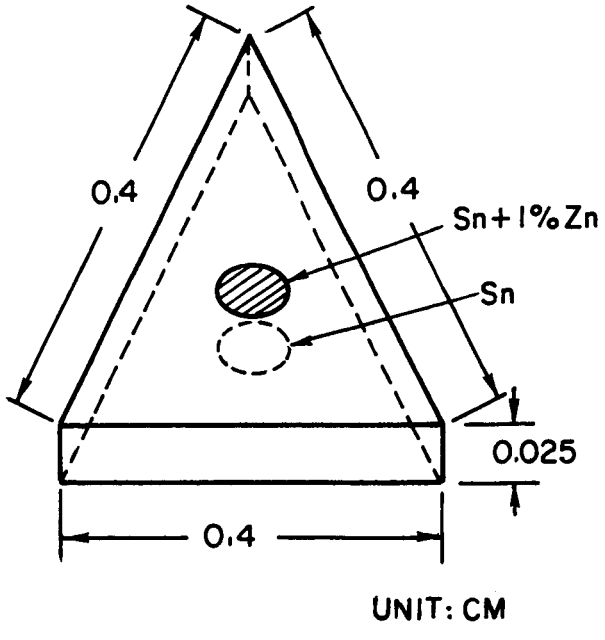

FIG. 5

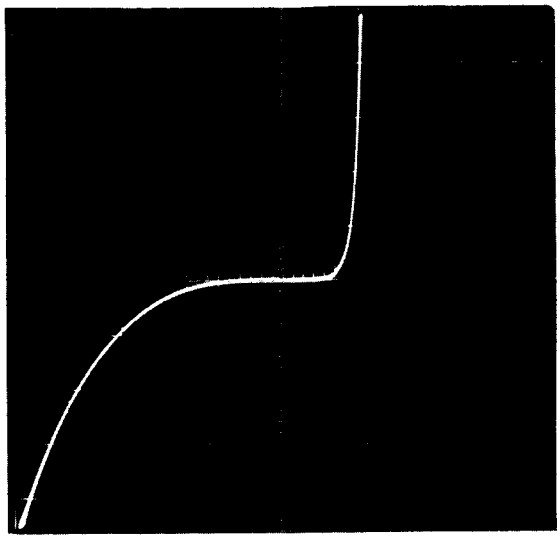

FIG. 6

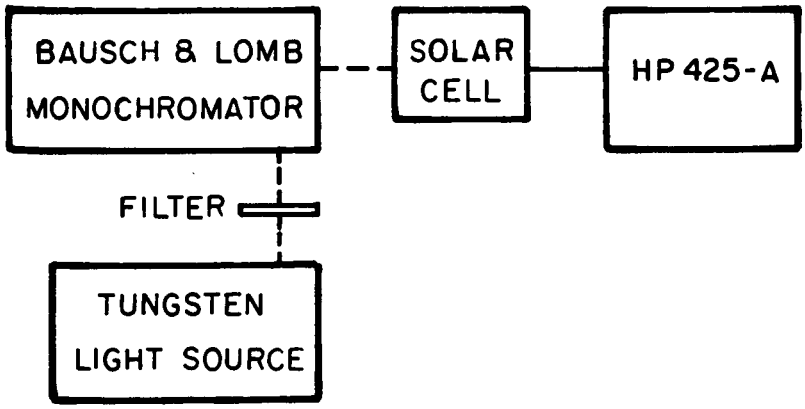
BAUSCH & LOMB
MONOCHROMATOR
SOLAR
CELL
HP 425-A
FILTER
TUNGSTEN
LIGHT SOURCE

FIG. 7

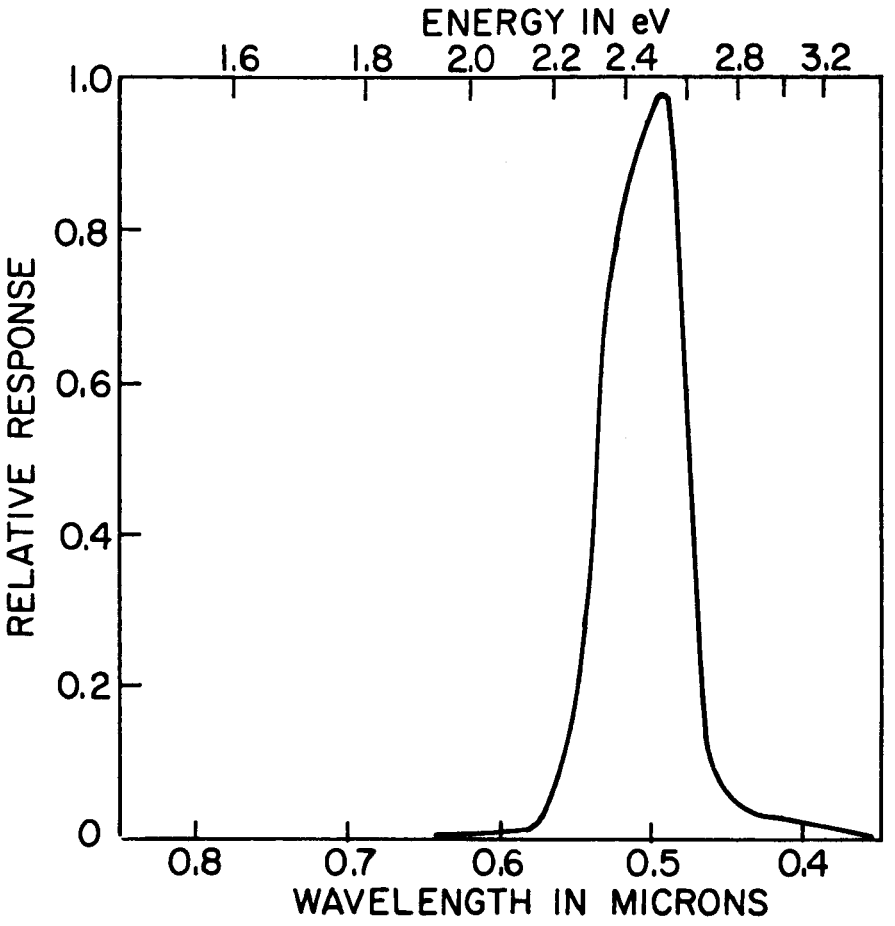
ENERGY IN eV
1.6
1.8
2.0
2.2
2.4
2.8
3.2
1.0
0.8
0.6
0.4
0.2
0
RELATIVE RESPONSE
0.8
0.7
0.6
0.5
0.4
WAVELENGTH IN MICRONS

FIG. 8

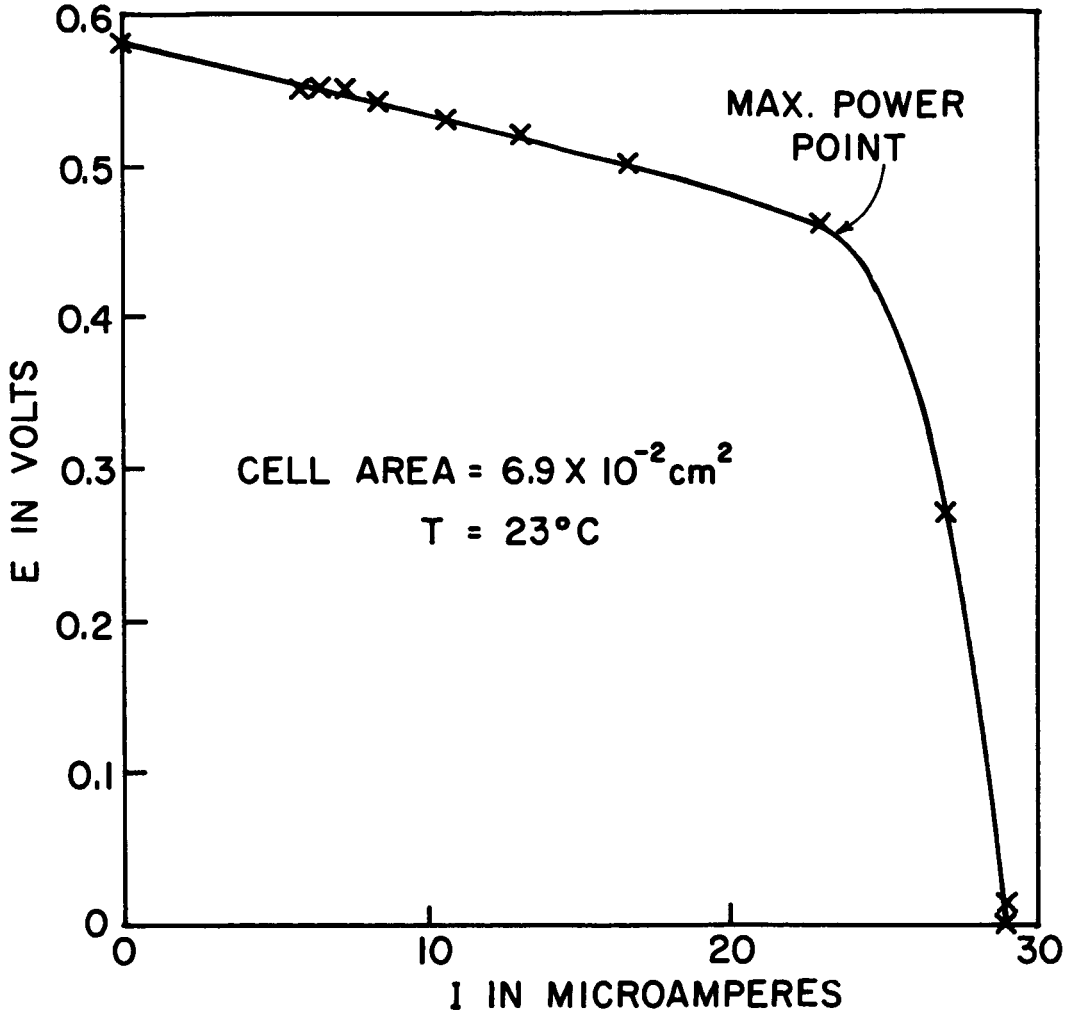
0.6
0.5
0.4
0.3
0.2
0.1
0
E IN VOLTS
MAX. POWER
POINT
CELL AREA = 6.9 X 10^-2 cm^2
T = 23°C
0
10
20
30
I IN MICROAMPERES

FIG. 9

PROJECT 5114: SEMICONDUCTING PROPERTIES OF GALLIUM PHOSPHIDE

National Aeronautics and Space Administration
Grant NsG-555
Project Leader: G. L. Pearson
Staff: J. W. Allen

The purpose of this project is to study the properties of GaP and $GaAs_xP_{1-x}$ relevant to their use as semiconducting materials.

Crystal field theory is a highly-developed method of describing the properties of certain specific types of impurities in crystalline solids. Most experimental work has been performed on ionic materials or on molecular complexes. In the past few years transition metal ions in II-VI compounds have been studied from the crystal field point of view. Recently we have been applying the method to the study of deep-lying impurity levels in III-V semiconductors.

In a previous Quarterly Research Review, No. 11, it was reported that the optical absorption of Fe, Co and Ni in GaP could be interpreted as arising from the d^6, d^7 and d^8 configurations respectively, thus showing the applicability of crystal field theory to this type of compound. In other III-V and group IV semiconductors the band gap is too small to allow the observation of optical absorption spectra arising from d-d transitions. It is therefore necessary to find correlations between impurity paramters and known properties of the host crystal. As examples, two such correlations will be presented here.

Matamura[1] suggested that the hyperfine constant A for divalent $Mn(d^5)$ is related to the ionicity of the crystal. This idea can be extended by relating A to the anion electronegativity, as shown in

Fig. 1. Since both A and the electronegativity are measures of the extent to which electrons are drawn from the impurity onto the surrounding ligands it is not surprising that a correlation exists; what is gratifying is that this correlation produces a smooth curve, showing that the bonding characteristic varies smoothly through the zinc-blende structure semiconductors.

In the second example, the reduction of the Racah parameter B in the crystal relative to the free ion value, denoted by the ratio $\beta \equiv B_{crystal}/B_{free\ ion}$, can be correlated with the refractive index of the host crystal, as shown in Fig. 2. This relation is particularly important since it allows us to estimate β in crystals in which the optical absorption due to the impurity cannot be observed.

It appears from this work that the crystal field approach provides a fruitful method of studying transition metal impurities in semiconductors, and the existence of correlations of the type described allows us to make quantitative estimates of some properties of such impurities which are otherwise not easily obtained by experiment.

REFERENCES

1. O. Matamura, J. Phys. Soc. Japan, 14, 108 (1959).

FIGURE CAPTIONS

Fig. 1 Correlation between the hyperfine constant A for $Mn(d^5)$ and electronegativity of the crystal anion.

Fig. 2 Correlation between the Racah paramter reduction ratio and the reciprocal square refractive index of the host crystal.

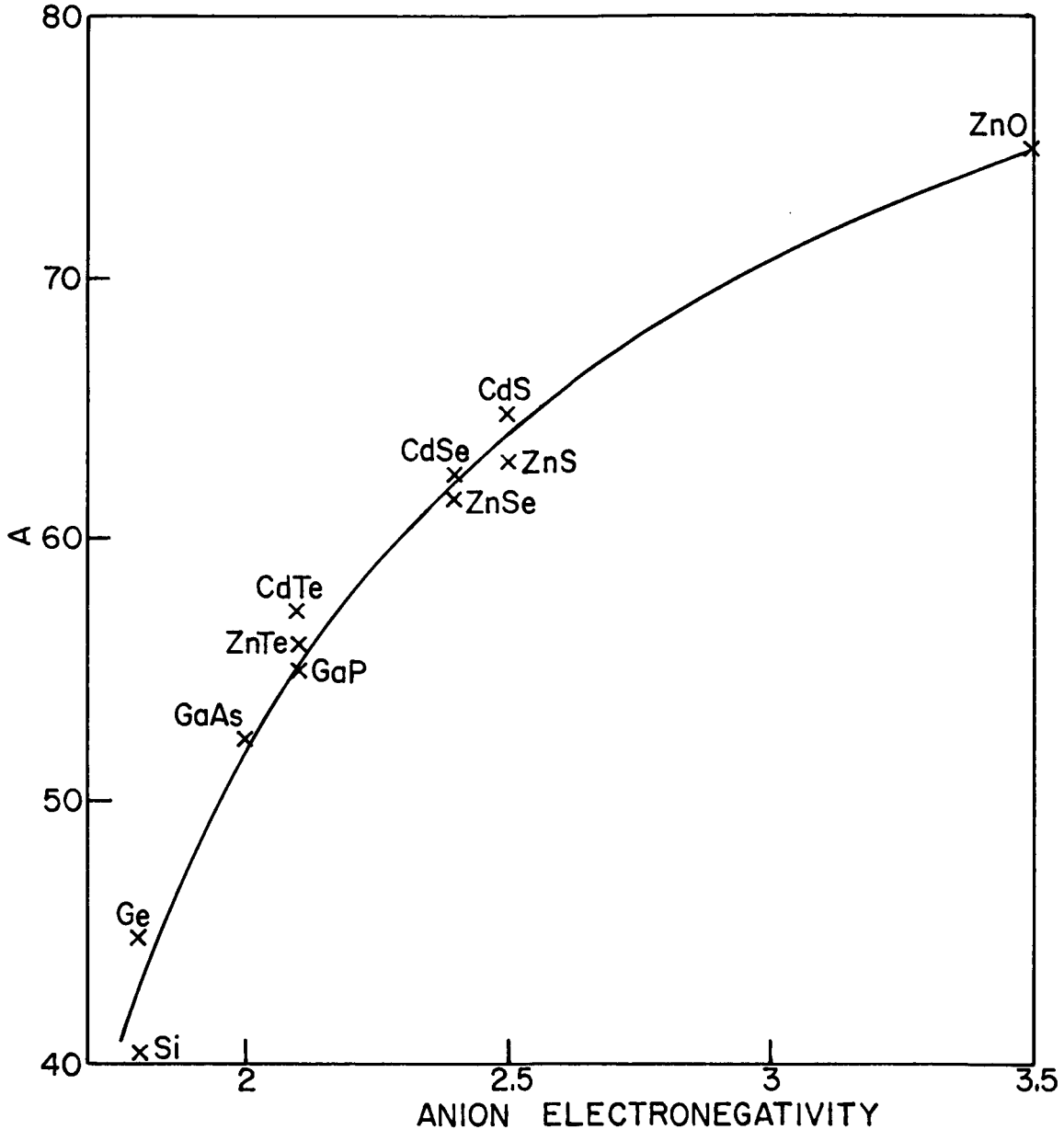
80
70
60
50
40
A
ZnO
CdS
CdSe
ZnS
ZnSe
CdTe
ZnTe
GaP
GaAs
Ge
Si
2
2.5
3
3.5
ANION ELECTRONEGATIVITY

FIG. 1

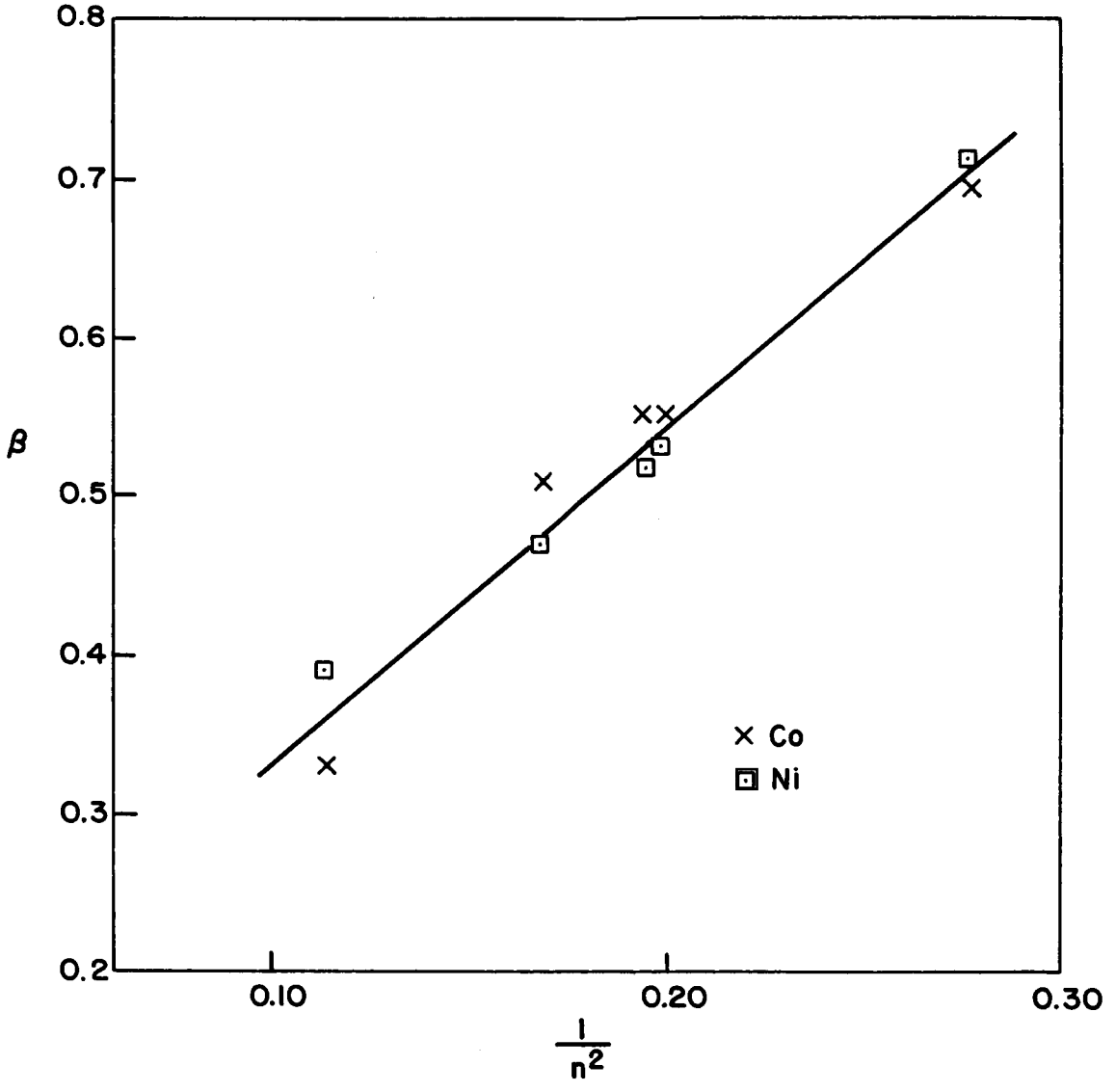

FIG. 2